Vision Research 50 (2010) 1328–1337

Contents lists available at ScienceDirect

Vision Research

journal homepage: www.elsevier.com/locate/visres

The spatial distribution of receptive field changes in a model of peri-saccadic perception: Predictive remapping and shifts towards the saccade target

Marc Zirnsak [a], Markus Lappe [a,b], Fred H. Hamker [a,b,c,*]

[a] Department of Psychology, Institute II, Westf. Wilhelms-University, Münster, Germany
[b] Otto Creutzfeldt Center for Cognitive and Behavioral Neuroscience, Münster, Germany
[c] Department of Computer Science, Artificial Intelligence, Chemnitz University of Technology, Germany

ARTICLE INFO

Article history:
Received 8 July 2009
Received in revised form 28 January 2010

Keywords:
Attention
Oculomotor feedback
Predictive remapping
Receptive field shifts
Saccade

ABSTRACT

At the time of an impending saccade receptive fields (RFs) undergo dynamic changes, that is, their spatial profile is altered. This phenomenon has been observed in several monkey visual areas. Although their link to eye movements is obvious, neither the exact pattern nor their function is fully clear. Several RF shifts have been interpreted in terms of predictive remapping mediating visual stability. In particular, even prior to saccade onset some cells become responsive to stimuli presented in their future, post-saccadic RF. In visual area V4, however, the overall effect of RF dynamics consists of a shrinkage and shift of RFs towards the saccade target. These observations have been linked to a pre-saccadically enhanced processing of the future fixation. In order to better understand these seemingly different outcomes, we analyzed the RF shifts predicted by a recently proposed computational model of peri-saccadic perception (Hamker, Zirnsak, Calow, & Lappe, 2008). This model unifies peri-saccadic compression, pre-saccadic attention shifts, and peri-saccadic receptive field dynamics in a common framework of oculomotor reentry signals in extrastriate visual cortical maps. According to the simulations that we present in the current paper, a spatially selective oculomotor feedback signal leads to RF dynamics which are both consistent with the observations made in studies aiming to investigate predictive remapping and saccade target shifts. Thus, the seemingly distinct experimental observations could be grounded in the same neural mechanism leading to different RF dynamics dependent on the location of the RF in visual space.
© 2010 Elsevier Ltd. All rights reserved.

1. Introduction

The classical receptive field (RF) of a visual cell is defined as the region in visual space where a stimulus has to be presented to drive the cell. In retinocentric areas this region depends on the eyes' position, that is, the RF is fixed in retinal coordinates but covers different parts of visual space during different fixations of the eyes. Since we constantly scan our environment by rapid eye movements called saccades, the input of cells in early visual to mid-level areas constantly changes. In order to construct an apparently stable and continuous percept of the world across saccades, it has been hypothesized that retinocentric representations are updated prior to the gaze shift (Duhamel, Colby, & Goldberg, 1992; Melcher & Colby, 2008; Wurtz, 2008). Indeed it seems that immediately before a saccade, cells in several brain areas transiently change the location and extension of their RF, that is, their RF profile is altered.

According to the conception of predictive remapping (Duhamel et al., 1992), a motor-related signal from the plan to move the eyes – known as corollary discharge – provides the visual system the necessary information to shift the RFs in retinocentric maps to the post-saccadic RF location (Sommer & Wurtz, 2006). Even prior to saccade onset cells become responsive to stimuli presented in their so-called future RF (FRF) (Fig. 1A). This phenomenon has been observed in monkey lateral intraparietal area (LIP) (Duhamel et al., 1992), superior colliculus (SC) (Walker, Fitzgibbon, & Goldberg, 1995), the frontal eye field (FEF) (Sommer & Wurtz, 2006; Umeno & Goldberg, 1997), and even in earlier visual areas like V3 and V3a (Nakamura & Colby, 2002).

Measurements in monkey V4 have also revealed that RFs change around the time of a saccade (Tolias et al., 2001). Like the RF dynamics described above, these RF changes begin prior to saccade onset, but the spatial pattern is different. Instead of a translation of the RFs parallel to the saccade, the overall effect rather shows a shrinkage and shift of RFs towards the saccade target (Fig. 1B), which suggests that before the eye movement the region around the saccade target is already processed by a greater amount of finer tuned RFs enabling the visual system to process the future fixation in greater detail.

* Corresponding author. Address: Künstliche Intelligenz, Informatik, Chemnitz University of Technology, Straße der Nationen 62, 09107 Chemnitz, Germany. Tel.: +49 251 83 34125.
E-mail address: fred.hamker@informatik.tu-chemnitz.de (F.H. Hamker).

0042-6989/$ - see front matter © 2010 Elsevier Ltd. All rights reserved.
doi:10.1016/j.visres.2010.02.002

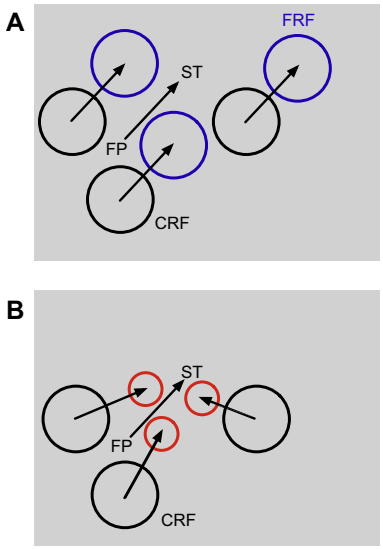

Fig. 1. Illustration of the two RF dynamics. Three hypothetical example cells are shown. Their current RFs (CRF), as measured during fixation or long before a saccade, are plotted in black. FP denotes the fixation point and ST the saccade target. (A) Conception of predictive remapping. Before saccade onset RFs are shifted to the location of the future RF (FRF). (B) V4 RF dynamics. Before saccade onset RFs shrink and shift towards the saccade target.

A simple conclusion drawn from these two apparently different observations could be that the peri-saccadic RF dynamics in V4 are fundamentally different from those in the other areas as mentioned above. However, in contrast to the recordings in V4, where the attempt was made to measure the complete RF profile, none of the existing remapping studies have provided such detailed measurements. Instead, the translation of RFs to their post-saccadic positions is extrapolated from a few visual probes (see Section 2 for details). In the following we will argue that both RF dynamics, that is, predictive remapping and the observed V4 RF shifts, can be caused by a single mechanism: a spatially selective, oculomotor related signal which is fed back into visual areas.

We start our line of arguments with a model of attention (Hamker, 2003, 2005a). According to this model, a spatially selective feedback signal modulates processing in visual areas. This signal emerges during spatial selection, is linked to the saccade target plan, and is suggested to arise in oculomotor areas like the FEF (Armstrong, Fitzgerald, & Moore, 2006; Armstrong & Moore, 2007; Pouget et al., 2009) or the SC (Cavanaugh & Wurtz, 2004; Müller, Philiastides, & Newsome, 2005). This model conception is consistent with the observation that neural responses are pre-saccadically enhanced if a saccade is directed towards a stimulus within their RF (Fischer & Boch, 1981a, 1981b; Mazer & Gallant, 2003; Moore, Tolias, & Schiller, 1998) and with psychophysical findings suggesting that spatial attention precedes an eye movement and immediately before saccade onset, is locked at the saccade target where visual performance is increased (Hoffman & Subramaniam, 1995; Kowler, Anderson, Dosher, & Blaser, 1995; Deubel & Schneider, 1996; Godijn & Pratt, 2002; Peterson, Kramer, & Irwin, 2004; Shepherd, Findlay, & Hockey, 1986). In further model extensions we have shown that the model also predicts dynamic RF changes by local gain modulations, i.e., the space dependent shape of the feedback leads to a non-uniform gain change and thus to a distortion in the population response (Hamker & Zirnsak, 2006; Hamker et al., 2008). In Hamker and Zirnsak (2006) this model was applied to shed light on the dynamics of V4 RF changes on a fine temporal scale. Model simulations revealed similar dynamics as reported by Tolias et al. (2001).

In Hamker et al. (2008) we have formalized the earlier concepts into a detailed model of hierarchical processing considering cortical magnification and the change in RF size across eccentricity to fit the model to behavioral data of experiments dealing with the peri-saccadic mislocalization of stimulus position (Ross, Morrone, & Burr, 1997). In these experiments a briefly presented stimulus is mislocalized towards the saccade target if shown around the onset of a saccade. Thus, this model explains this phenomenon, also known as peri-saccadic compression, as a consequence to shift processing resources towards the future eye position before the eye starts to move. A first analysis of its predicted RF changes showed a variety of responses. Among those are some that seem both consistent with the reported V4 dynamics, that is, a shrinkage and shift towards the saccade target, and, although not explicitly implemented in the model [see Quaia, Optican, and Goldberg (1998) for an explicit implementation of remapping], with the predictive remapping conception, that is, a shift of RFs parallel to the saccade. In the present study we performed an in depth RF analysis of the model predictions. We computed the predicted RF change for each cell dependent on the classical RF center in visual space. This allows us to estimate the RF changes that can be expected by oculomotor feedback during eye movements and to compare them to the reported RF changes by applying systematically the methods which have been used to assess the RF dynamics in different brain areas.

2. Methods

2.1. Model of peri-saccadic perception

In this section we give a short description of the model. For details, please refer to Hamker et al. (2008). As illustrated in Fig. 2, a single area of the visual hierarchy is modeled by three functional stages. The input stage represents "simple" cells for feature detection. They project via the gain stage, in which the supposed feedback signal acts, to the so-called pooling stage consisting of "complex" cells, which share the same feature space as simple cells but possess an increased spatial invariance. Long before saccade onset, there is no feedback signal and the activity of the gain stage will be identical to the input stage. However, in the presence of a feedback signal the activity of the gain layer is modulated. As stated above, the feedback signal is supposed to arise in oculomotor areas like the FEF and the SC. In analogy to cells in these areas the feedback signal in the model builds up before the saccade and reaches its maximal strength at saccade onset. According to its spatial properties, the feedback signal is described as a gaussian distribution in cortical space centered at the representation of the saccade target. As a result, cells which are located in cortical space closer to the saccade target, are subject to stronger gain modulations than cells which are located farther away from the feedback center, which is consistent with electrophysiological observations (Armstrong et al., 2006). In total, these gain changes cause population responses being distorted towards the center of the feedback. "Reading out" these distorted populations leads to the prediction of a mislocalization pattern which resembles a compressed visual space. This means, stimuli which are presented to the model in the context of a strong feedback signal, that is, at the time of an impending saccade, are localized closer towards the saccade target. Thus, mislocalization is the result of an asymmetric change in gain and not due to a gain change per se. Furthermore, cells which are driven by these distorted populations show an altered RF.

A possible relation between spatial distortions and RF changes has been proposed earlier by Suzuki and Cavanagh (1997) to explain mislocalization of stimuli observed during covert shifts of attention. This study found that subjects reported a briefly pre-

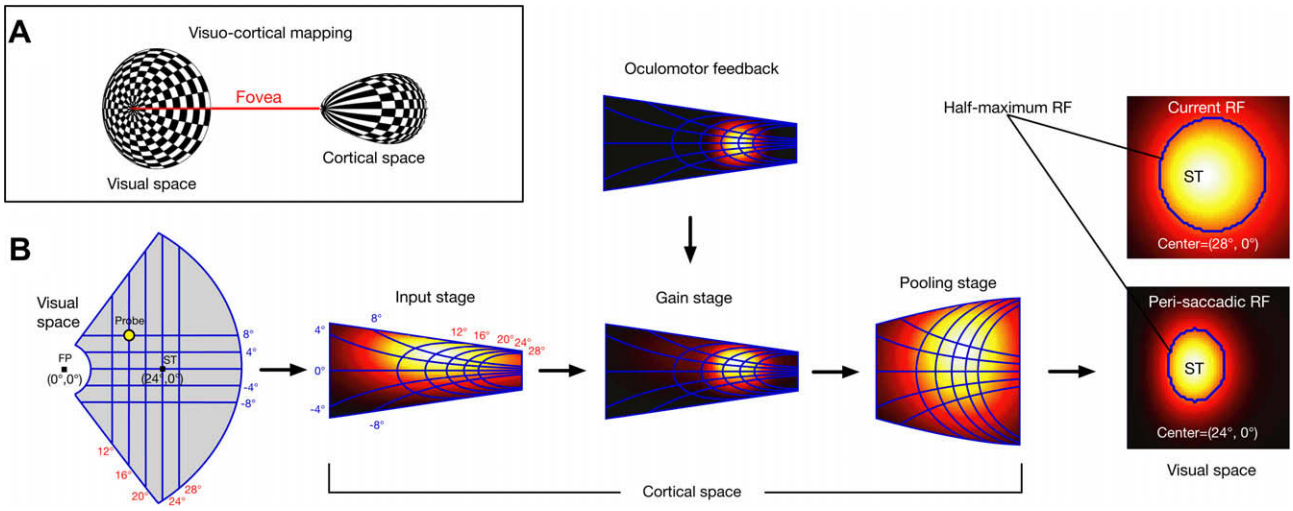

Fig. 2. Illustration of the model. (A) The visual space, described in spherical coordinates, is mapped into cortical space according to cortical magnification factors. (B) A visual area in the model consists of an input stage, a gain stage, and a pooling stage. The input stage encompasses the unmodulated population activity caused by a probe presented in visual space. If there is no feedback signal, the activity of the gain stage will be equal to the input stage, which is true for the fixation condition. In the peri-saccadic condition the population of the gain stage gets distorted towards the saccade target by the impact of the oculomotor feedback signal, which also leads to changes in the RFs of cells in the pooling stage as it is illustrated on the right by the half-maximum profiles.

sented vernier stimulus to be offset away from a preceding cue stimulus that captured attention. To explain these results the authors assumed several scenarios of attention induced RF changes and the consequences of the latter on the population response.

While the latter principle is in general similar to our account it differs in some important aspects. Most importantly in our model we neither assume explicitly certain types of RF changes to induce distorted population responses nor do we use these parameters to fit the model to behavioral data. Instead, we simulate neurophysiological plausible gain changes in a hierarchical processing architecture as already described above. Both the distortion of neural population responses and RF changes in our model are the consequences of these gain changes. Without taking into account properties of cortical space, that is, an unequal sampling of visual space as a function of cortical magnification factors, this mechanism would lead to RF shifts directed towards the center of the feedback signal (Compte & Wang, 2006; Womelsdorf, Anton-Erxleben, & Treue, 2008). In Hamker et al. (2008) we found that the asymmetrical two-dimensional compression pattern obtained by Kaiser and Lappe (2004) could only be reasonably explained by assuming an anisotropic mapping of cortical space for early visual areas (Adams & Horton, 2003; Schira, Wade, & Tyler, 2007; Van Essen, Newsome, & Maunsell, 1984) assuming that the feedback is a gaussian in cortical space. This property also leads to asymmetrical RF changes in the model, since the feedback signal in visual space is elongated along the circles of constant eccentricity, resulting in our previous observation that while certain cells seem to be consistent with the predictive remapping literature, others showed changes strongly reminiscent of the reported V4 dynamics. Note, that the anisotropic mapping of visual space has not necessarily to be property of all model stages to obtain our findings. In fact, only the input stage and gain stage, which share the "same" cortical space, are subject to anisotropy, however, the pooling stage, for which all subsequent RF dynamics are reported, possesses an isotropic cortical space.

For all simulations described below we used the same model parameters as described in Hamker et al. (2008). In that study the model was fitted to the experimentally observed peri-saccadic mislocalization data reported in Morrone, Ross, and Burr (1997) and Kaiser and Lappe (2004). As a result, we obtained parameter estimates of four saccade amplitudes (12°, 16°, 20°, 24°) which were used in this study. Thus, we will analyze the inherent RF changes of a model fitted to behavioral data. Again note, we did not assume certain types of RF dynamics to fit the model to the data.

Consistent with neuroanatomical findings the size of model RFs increases with eccentricity and the distribution of cells is highest in the fovea and decreases with eccentricity according to cortical magnification factors as already described above. With respect to these parameters the simulated model area is comparable to monkey areas like V4, V3a and the middle temporal area (MT).

For the purpose of this study we mapped the model RFs in two conditions. In the first condition, which we call the fixation condition, we mapped the current RFs (CRFs). This mapping was done pre-saccadically long before saccade onset (without an oculomotor feedback signal). In the second condition the mapping was done immediately before saccade onset when the feedback signal was strong. We will call this the peri-saccadic condition.

2.2. Changes in RF size

To assess the change in RF size, we applied the same response rule, which was used by Tolias et al. (2001). That is, for a given neuron we determined its RF in both the fixation and peri-saccadic condition by stimuli, in the following referred to as probes, eliciting a response which has to be higher than half of the maximum response of the neuron. The change of RF size Δs_{RF}, that is, the area of the half-maximum profile, between the fixation and the peri-saccadic condition was then obtained by

$$\Delta s_{RF} = 100 \frac{s_{RF}^{peri} - s_{RF}^{fix}}{s_{RF}^{fix}},$$

where s_{RF}^{peri} and s_{RF}^{fix} denote the half-maximum RF size of a given cell in the peri-saccadic condition and the fixation condition, respectively.

2.3. Changes in the number of responsive cells

To assess the overall effect of the RF changes due to changes in position or size, the number of cells responding effectively to a probe at a certain location was compared between the fixation

and the peri-saccadic condition as follows. For a given probe location in visual space the number of cells whose responses exceeded the half of the maximum activity of the respective cell, in the following referred to as responsive cell, was computed for the fixation condition and the peri-saccadic condition to determine the peri-saccadic change in the number of responsive cells as a function of spatial location.

$$\Delta n_{RF} = 100\frac{n_{RF}^{peri} - n_{RF}^{fix}}{n_{RF}^{fix}},$$

where n_{RF}^{peri} and n_{RF}^{fix} denote the number of responsive cells for a given location in visual space in the peri-saccadic condition and the fixation condition, respectively.

2.4. One-probe remapping test

To evaluate the consistency of the RF changes in the model with predictive remapping we applied three tests. The first test is the most common method in the literature (Duhamel et al., 1992; Nakamura & Colby, 2002; Umeno & Goldberg, 1997; Walker et al., 1995). It consists of placing a single probe in the center of the FRF of a given cell (Fig. 3A). The FRF is the region in visual space where the CRF will be located after the eye movement. The cell is classified as a predictive remapping cell, if the probe activates the cell already before the eye movement or if the latency of the response is shorter than the latency that would be expected for the CRF during fixation. In the model, all reported RFs were measured before saccade onset since the model is static. In the following we will refer to this test as the one-probe test. Note that in the electrophysiological studies usually cells are selected which do not respond above baseline to a probe presented in the FRF during the fixation task. The response of such a cell to a probe in the FRF during the saccade task has to be significantly different from baseline activity to be considered as a remapping cell. Since the model is noiseless, we cannot directly apply this statistical procedure. We labeled a cell as a remapping cell in the one-probe test, if the activity to a probe in the FRF during the saccade task, that is, the peri-saccadic condition, increased at least by 5% relative to the maximum activity in the fixation condition.

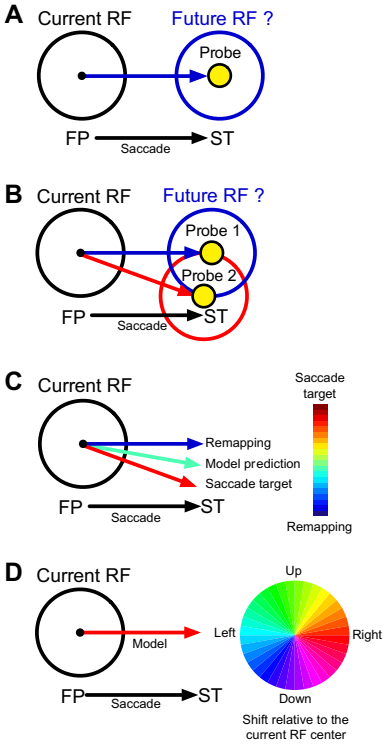

Fig. 3. Illustration of the applied tests and measures. (A) One-probe test. (B) Two-probe test. (C) Continuous remapping test. (D) Shift direction of the maximum activity increase of the peri-saccadic RF at p_{max} relative to the CRF center.

2.5. Two-probe remapping test

The second test was introduced by Sommer and Wurtz (2006) and was designed to differentiate between remapping and saccade target shifts. It uses two probes. As in the one-probe test, the first probe is presented in the center of the FRF. The second probe is placed close to the saccade target (Fig. 3B), to test for RF shifts towards the saccade target. If the RF translates parallel to the saccade, the first probe should evoke a stronger activation of a neuron as compared to the second probe. If the RF shifts towards the saccade target, the second probe should evoke a stronger activation of a neuron than the first probe. We will refer to this test as the two-probe test. In the model we compared the activity increase of a cell to a probe in the FRF to the activity increase to a probe presented closer to the saccade target, that is, to a probe which was placed at the endpoint of a vector pointing directly towards the saccade target. The origin of this vector is equal to the center of the CRF and its magnitude is equal to the saccade amplitude. If the distance between the CRF center and the saccade target was shorter than the saccade amplitude, the probe was presented directly at the saccade target location. As in the one-probe test, to be considered as a significant change a probe had to cause at least an activity increase of 5% relative to the maximum activity in the fixation condition. If the activity increase to a probe in the FRF was higher than the activity increase to a probe presented closer to the saccade target, it was classified as a remapping cell.

2.6. Continuous remapping test

The above procedures for RF mapping in the model match the typical procedures used in electrophysiological experiments as closely as possible. However, with the model we also have the possibility to use procedures that cannot reasonably be performed in electrophysiological experiments due to time or method restrictions. While such procedures do not allow a direct comparison to physiological data, they can be very useful to illustrate the mechanism at work. We therefore included an additional remapping test. For each cell we determined the location where the increase of the peri-saccadic RF as compared to the fixation RF is maximal

$$p_{max} = \arg\max_{p_i}\left(r^{peri}(p_i) - r^{fix}(p_i)\right),$$

where r^{peri} and r^{fix} denote the activity for a given cell to a probe presented at position p_i for the peri-saccadic and the fixation condition, respectively. To be considered as a significant shift in RF profile, the maximum activity increase p_{max} had at least to be 5% of the maximum activity in the fixation condition. We then computed a displacement vector $\mathbf{v}$ with the CRF center as origin and p_{max} as endpoint. When the magnitude of this vector was greater than 1°, the direction ϕ_v of $\mathbf{v}$ was compared to the direction predicted by remapping ϕ_R and to the direction pointing directly towards the saccade target ϕ_{ST}, that is, we determined the minimal angle ϕ_{min} between ϕ_v and ϕ_R, and between ϕ_v and ϕ_{ST}, with

$$\phi_{min} = f(\phi_1, \phi_2) = \begin{cases} 2\pi - |\phi_1 - \phi_2| & \text{if } |\phi_1 - \phi_2| > \pi \\ |\phi_1 - \phi_2| & \text{else} \end{cases}.$$

These angles were then used to compute a shift index

$$S = \frac{f(\phi_v, \phi_R)}{f(\phi_v, \phi_R) + f(\phi_v, \phi_{ST})},$$

where $S \in [0, 1]$ indicates the relative similarity between ϕ_v and ϕ_{ST}, respectively the similarity between ϕ_v and ϕ_R, with $S = 1$ if $\phi_v = \phi_{ST}$ and $S = 0$ if $\phi_v = \phi_R$ (Fig. 3C).

3. Results

3.1. Changes in RF size

Changes in the RF profile depend on a function of the CRF center relative to the saccade target, the CRF size, and the saccade amplitude. Fig. 4 shows the amount of size change (shrinkage or expansion) of RFs in the peri-saccadic condition for the four saccade amplitudes (12°, 16°, 20°, 24°) together with examples of half-maximum profiles of typical cells. The general pattern is similar for all simulated amplitudes. In the region right and above the saccade target, cells with CRF centers relatively close to the saccade target have smaller RFs (blue regions) in the peri-saccadic case, while cells farther away show an expansion of their RFs (red regions). Thereby, for all saccade amplitudes the expansion is largest for cells with CRF centers located around the region of the fixation point. Between these cells showing expansion and shrinkage, there are cells which do not alter in RF size (enclosed white regions), but nevertheless show a translation (e.g., see the cell with its CRF center at $x = 4°$ and $y = 16°$ for a 20° saccade). The majority of cells with CRF centers located in the opposite hemisphere relative to the saccade target location do not show any change in their RF profile which is more prominent for the 20° and 24° saccade as compared to the 12° and the 16° saccade. The RF size of cells with their CRF centers located close to the fixation point is too small to be affected by the feedback signal of the 20° and 24° saccade. For the 12° and 16° saccade, however, the same cells are sufficiently close to the feedback signal so that their RF properties are now altered. In general, the resulting RF dynamics lead to peri-saccadic half-maximum profiles that are located closer to the saccade target in comparison to their CRF profiles of the fixation condition (please also refer to the shift direction and amplitude of the continuous remapping test shown in Fig. 8).

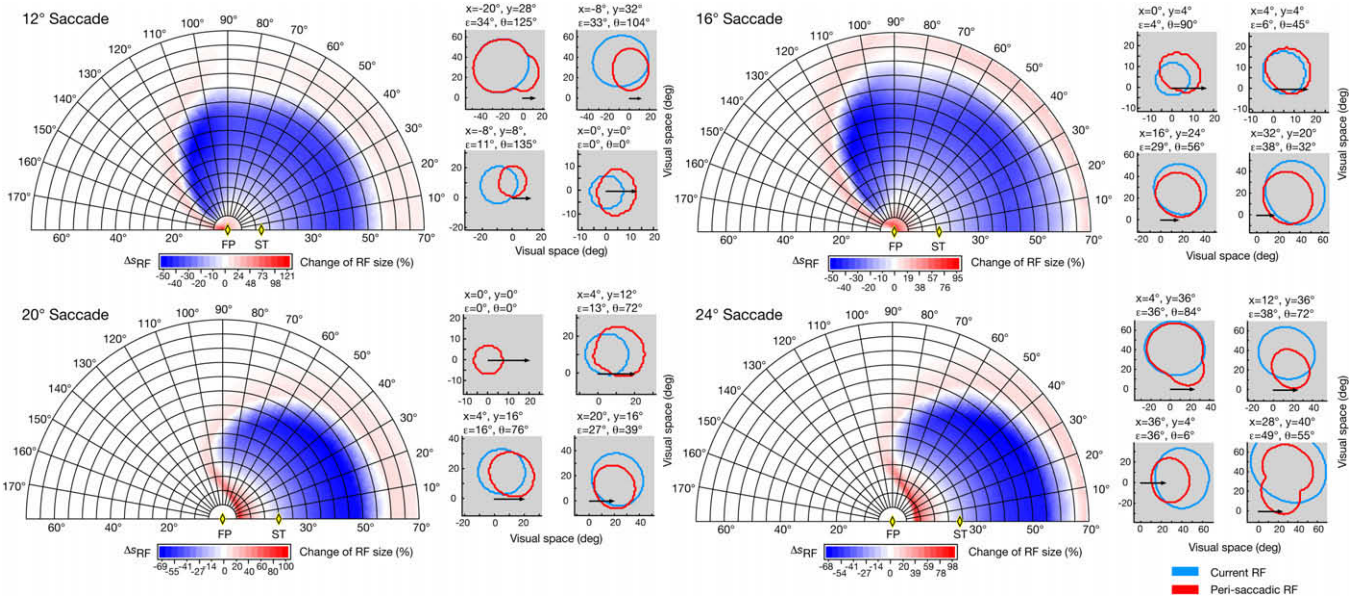

Fig. 4. Changes in the size of peri-saccadic RFs (Δs_{RF}) shown as a function of the CRF center in visual space displayed together with representative half-maximum RF profiles. Since the results of the lower part of visual space are identical to the results of the upper part of visual space for all reported simulations (see Fig. 5), only the upper part of visual space is shown. An expansion of RFs is indicated in red and a shrinkage of RFs is indicated in blue. Fixation and peri-saccadic half-maximum profiles are shown in light blue and red, respectively. The center of the CRF is given in Cartesian (x, y) and Polar (ϵ, θ) coordinates. Yellow diamonds indicate the fixation point (FP) and the saccade target (ST).

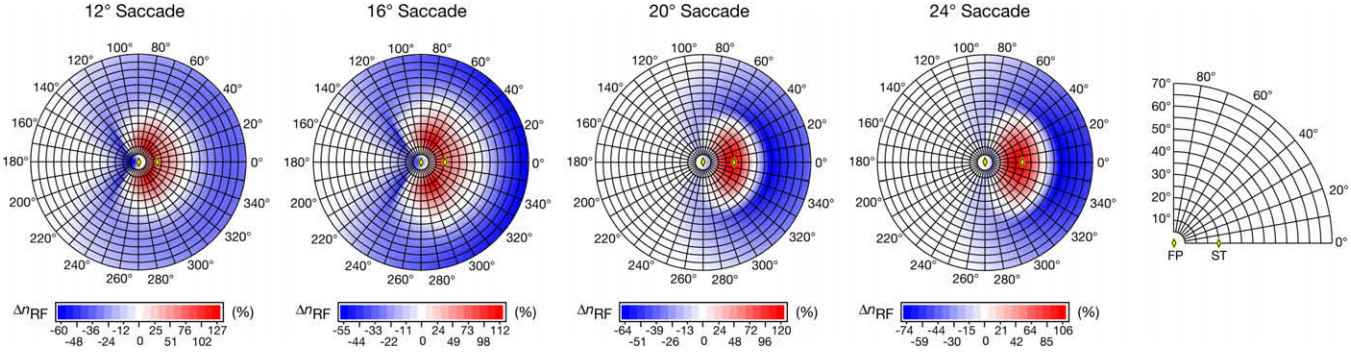

Fig. 5. Distributions of the peri-saccadic change in the number of responsive cells (Δn_{RF}) as a function of probe position in visual space. Yellow diamonds indicate the fixation point (FP) and the saccade target (ST). An increase in the number of responsive cells is indicated in red and a decrease in blue. (For interpretation of the references to color in this figure legend, the reader is referred to the web version of this article.)

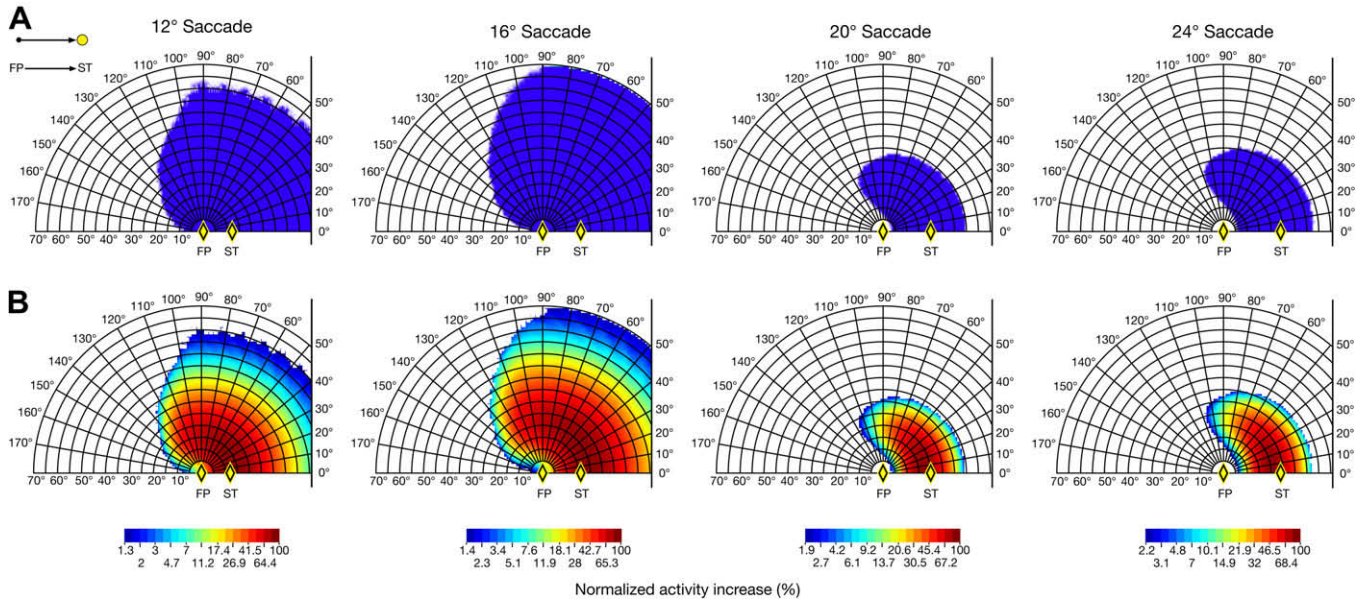

Fig. 6. Results of the one-probe test. (A) The blue area consists of the positions of CRF centers in visual space where cells are classified as predictive remapping cells. (B) Peri-saccadic activity increase shown as a function of the CRF center in visual space. Note that the activity increase was normalized for each condition, that is, each saccade amplitude. Yellow diamonds indicate the fixation point (FP) and the saccade target (ST). (For interpretation of the references to color in this figure legend, the reader is referred to the web version of this article.)

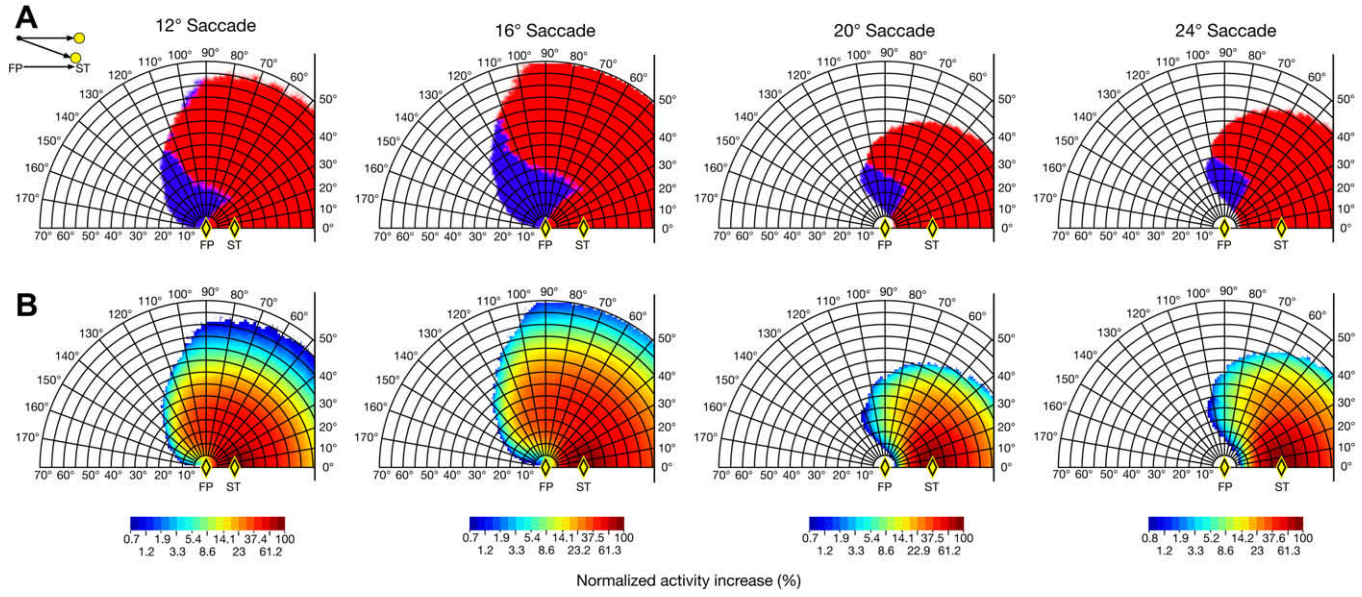

Fig. 7. Results of the two-probe test. (A) The blue area consists of positions of CRF centers in visual space where cells are classified as predictive remapping cells. The red area consists of the positions of CRF centers in visual space where cells respond more strongly to the probe which is presented in direction to the saccade target. (B) Peri-saccadic activity increase shown as a function of the CRF center in visual space. Yellow diamonds indicate the fixation point (FP) and the saccade target (ST). (For interpretation of the references to color in this figure legend, the reader is referred to the web version of this article.)

3.2. Changes in the number of responsive cells

The changes in the number of responsive cells are summarized in Fig. 5. For all saccade amplitudes the number of responsive cells increases (red regions) at the saccade target and at nearby regions (up to 127%) and decreases (blue regions) at surrounding positions (down to −74%). Thus, in terms of the number of responsive cells the processing capacity is enhanced in the peri-saccadic condition at the saccade target region with the cost of a decreased processing capacity at surrounding regions (see also Hamker et al., 2008).

3.3. One-probe remapping test

The blue area in Fig. 6A denotes the region where cells are classified as remapping cells according to the one-probe test (see Section 2). Since the oculomotor feedback signal is broader for the 12° and the 16° saccade amplitude, the area where cells are affected by the feedback signal is larger than for the 20° and the 24° saccade. The increase of the activity of a given cell depends on its CRF center (Fig. 6B). Cells close to the center of the feedback signal, that is, the saccade target, show the largest increase in activity.

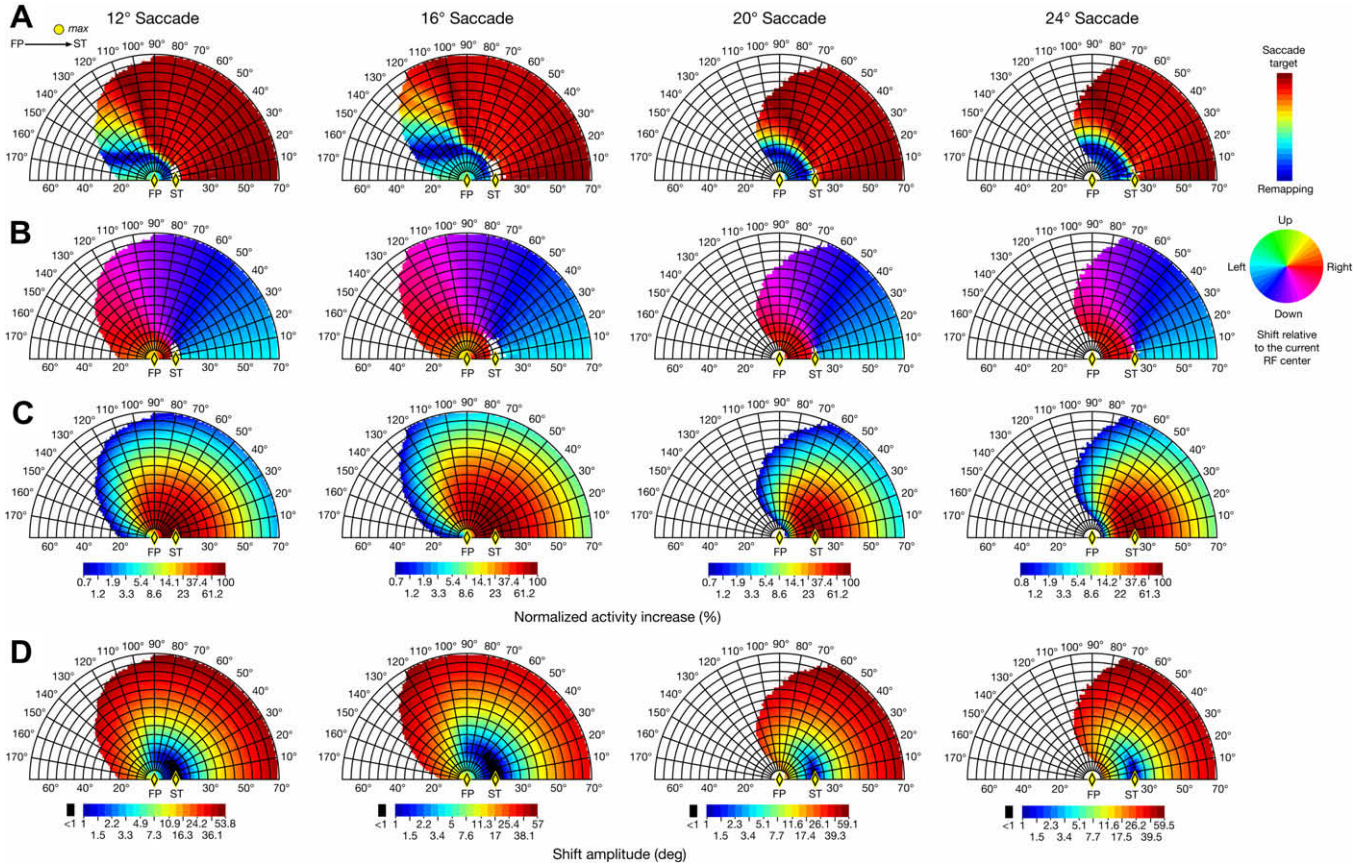

Fig. 8. Results of the continuous remapping test. (A) Visualization of the shift index *S*. (B) Shift direction of the maximum activity increase of the peri-saccadic RF relative to its CRF center. (C) Maximum peri-saccadic activity increase. (D) Shift magnitude of the maximum peri-saccadic activity increase. All measures are shown as a function of the CRF center in visual space. Yellow diamonds indicate the fixation point (FP) and the saccade target (ST). (For interpretation of the references to color in this figure legend, the reader is referred to the web version of this article.)

3.4. Two-probe remapping test

The two-probe test explores whether cells shift towards the saccade target or along the saccade vector (Sommer & Wurtz, 2006). In our model we observe both behaviors (Fig. 7). The region where cells are classified as remapping cells (blue area) is roughly the same for all saccadic amplitudes, that is, cells with their CRF centers located above the fixation point. Thus, the majority of RF positions, which are classified as remapping cells according to the one-probe test, do not pass the more sophisticated two-probe test. However, the remaining region of remapping cells seems consistent with the centers of remapping cells as reported in the literature. Fig. 7B shows the normalized increase of the activity of a given cell. The results are qualitatively the same as for the one-probe test (see above). Note that the activity increase is shown for the probe eliciting the higher response (see Methods), that is, for remapping cells (blue region in Fig. 7A) the activity increase depends on the probe that was presented in the FRF. For the rest of the cells (red region in Fig. 7A) the activity increase depends on the probe, which was presented closer to the saccade target.

3.5. Continuous remapping test

Fig. 8 shows the results of the continuous remapping test. As for the two-probe test, cells with a displacement direction close to the predicted remapping direction (dark blue regions in Fig. 8A) are located above the fixation point. In general, due to the different test condition (see Methods) the area of remapping cells is larger for the continuous test as compared to the two-probe test, which is especially true for the 20° and the 24° saccade. Yellow and light blue regions denote CRF centers for which the displacement direction lies in between the predicted remapping direction and the direction of a displacement towards the saccade target, whereas red regions denote a displacement direction pointing close towards the saccade target. Fig. 8B shows the displacement directions relative to the CRF center (see also Fig. 3D). As can be seen for the 12° and the 16° saccade for some cell positions close to the fixation point the displacement is actually directed more upwards (denoted in yellow) as would be expected by a predictive remapping displacement. Fig. 8C shows the maximum normalized increase of the activity of a given cell. The results are qualitatively the same as for the one-probe and the two-probe test. The increase is highest for cells with CRF centers located close to the saccade target. Fig. 8D shows the magnitude of the displacement. Although there are regions where cells show a displacement direction consistent with predictive remapping (Fig. 8A), the amplitudes of the shifts in these regions show larger variations as compared to a stringent remapping conception. Often the amplitudes are either smaller or larger than the saccade vector. Furthermore, cells with their CRF centers located close to the saccade target do not show a significant shift (>1°) at all.

4. Discussion

Physiological studies revealed different patterns of RF changes around the time of a saccade. RF changes parallel to the saccade vector are commonly referred to as remapping, presumably to gen-

erate a continuously accurate representation of visual space across eye movements (Duhamel et al., 1992; Nakamura & Colby, 2002; Sommer & Wurtz, 2006; Umeno & Goldberg, 1997; Walker et al., 1995). RF shifts towards the saccade target could be involved in enhancing information processing of relevant stimuli – those selected for detailed analysis by shifting gaze (Tolias et al., 2001). Are the peri-saccadic influences in V4 fundamentally different from those areas where cells have been classified as predictive remapping cells or might these differences depend on the selection of cells used for the analyses?

Our model shows a wide spectrum of RF dynamics. They consist of combinations of shrinkages, expansions, and shifts, (Fig. 4) which can in principle reproduce both the observed V4 dynamics and the RF effects of predictive remapping. The exact pattern of the simulated model dynamics depends on the center of the CRF and the saccade amplitude, confining the occurrence of particular types of RF dynamics to restricted regions of the visual field.

Our simulations suggest that the one-probe test, which has been used in most of the remapping studies (Duhamel et al., 1992; Nakamura & Colby, 2002; Umeno & Goldberg, 1997; Walker et al., 1995) cannot fully discriminate between predictive remapping and saccade target shifts. Many model cells that were classified as remapping cells according to the one-probe test did not pass the more sophisticated two-probe test. The two-probe test restricted the areas consistent with predictive remapping to a relatively small part of the visual space around the fixation point, which seems to correspond to areas where the CRF of cells in the above mentioned studies were located. Thus, the one-probe test in general might indicate whether a tested cell gets more responsive to a probe presented in its future receptive field, but it does not provide strong evidence for predictive remapping in the sense that cells globally shift along the saccade vector. Thus, an analysis of a subset of cells with RFs within a particular region of the visual field can, according to our model, lead to a severe bias with respect to the overall RF shift pattern.

This model prediction applies to all visual brain areas, which receive FEF inputs that implement a change in gain. While several brain areas receive input from the FEF (Schall, Morel, King, & Bullier, 1995), it is presently not clear if it always acts to change the gain as in V4 (Moore & Armstrong, 2003). However, it would not be surprising to find that other mid-level areas such as V3a, TEO, or MT were similarly influenced by the FEF. The processing in LIP, FEF, and SC might be more fundamentally different. That is, it might well be possible that both RF dynamics, the shifts induced by spatial feedback and those of predictive remapping, exist in parallel, but take place at different levels of the processing hierarchy. Areas like V3a, TEO, or MT might show similar effects as V4 in order to extract relevant features around the future fixation while areas like LIP of the parietal cortex might take part in an updating process. LIP is more involved in space perception rather than feature analysis and linked within the oculomotor network (Colby & Goldberg, 1999). Moreover, it plays a role in the transition from a retinocentric representation into other reference frames (Mullette-Gillman, Cohen, & Groh, 2005). Thus, the FEF could possibly affect LIP differently than V4. The FEF itself is known for saccade target selection including its reentrant processing within visual-oculomotor loops (Hamker & Zirnsak, 2006; Pouget et al., 2009) containing the SC. It remains to be investigated how the projections from the SC via the Thalamus exactly affect the neurons in the FEF, but the changes observed by Sommer and Wurtz (2006) could be consistent with a spatially selective change in gain or with additive inputs since the SC encodes the saccade target as well (Sommer & Wurtz, 2004).

Finally, it is not necessary that the gain modulations have to occur in the same areas in which they are observed, that is, higher areas, like LIP or FEF, will show similar dynamics if they are simply driven by distorted populations of earlier areas, for example V4 which is connected to both of the former mentioned areas (e.g., Ungerleider, Galkin, Desimone, & Gattass, 2008). Therefore, we suggest that the understanding of the RF dynamics of cells in the mentioned areas of the visual system benefits from an analysis that takes the location of the CRF in visual space systematically into account, that is, an analysis which describes the observed RF dynamics as a function of the CRF position and size. To our knowledge, this has yet neither been done for V4 nor for the areas that have been linked to predictive remapping, in particular LIP, FEF, SC, V3, and V3a. Such an analysis may reveal whether the experimentally observed RF dynamics might indeed be caused by the same mechanism as it is implemented in our model.

One might wonder if the all of this change in receptive fields around the time of saccades, which seems to involve an enormous effort and use of resources, would be needed if the only aim was to concentrate attention to the saccadic target. Indeed, a model of predictive remapping of receptive fields in LIP requires a massive interconnection as every neuron within LIP needs to be connected to every other LIP neuron in order to allow remapping in any saccade direction (Quaia et al., 1998). However, our model of receptive field dynamics actually requires comparatively little effort and resources since all effects are derived from modulatory feedback interactions that are restricted to the region around the saccade target. Thus, feedback connections from any oculomotor neuron are confined to the part of the map that surrounds the saccade amplitude of that neuron. No connectivity within the visual layer is required. Moreover, all connections in the model serve the general mechanism of the spatial deployment of attention. None are specifically added to induce receptive field shifts. Thus, receptive field changes in our model do not require any effort or resources other than those required for the purpose of directing attention.

Given the assumption that the model is true, several implications may be discussed. The most obvious implication is that instead of representing a global phenomenon, predictive remapping might be limited to a certain region of visual space, which depending on the type of measurement, roughly encompasses the region around the fixation point (two-probe and continuous remapping test) or the region between the fixation point and the saccade target (continuous remapping test). Although this conception seems reasonable with respect to the results of the two-probe test and the direction of the shift in the continuous remapping test, an in depth analysis of the RF dynamics leads to an even more complex picture. That is, although we observe cells shifting their RFs parallel to the saccade, the amplitude of these shifts indicates that the peri-saccadic RFs are located closer to the saccade target, similar as it is reported for cells in V4. Furthermore, part of these cells also show an expansion of their RFs (Fig. 4). Since we did not model inhibitory interactions we do not give particular emphasis on the detailed RF profiles, but the expansion observed in several cells is consistent with changes in the average RF reported in the FEF (Sommer & Wurtz, 2006). In this study, RFs do not undergo a complete translation as it is commonly associated with the predictive remapping conception but rather stretch or develop a bimodal profile in order to cover a greater amount of the saccade target region. Such bimodal profile can occur in the model if the feedback signal is sufficiently distant to the RF center. We would expect that these cells rather participate in an enhanced processing of the saccade target region, but do not update an internal reference frame which is often suggested to play an important role in visual stability (e.g. Wurtz, 2008).

While in general the conception of predictive remapping suggests a global account for spatial stability, others have stressed the importance of local visual information provided after a saccade. Both the saccade target theory (Currie, McConkie, Carlson-Radvansky, & Irwin, 2000; Irwin, McConkie, Carlson-Radvansky, & Currie, 1994; McConkie & Currie, 1996) and the object reference theory

(Deubel, Bridgeman, & Schneider, 1998; Deubel, Schneider, & Bridgeman, 1996) propose an important role of the saccade target. It is suggested that the visual system possesses a built-in stability assumption, which is only rejected if there is sufficient evidence for an alternative interpretation. Prior to an eye movement visual information at the future eye position is stored and compared to the visual input after the eyes have landed. If there is a reasonable match, perceived stability will be maintained. In this conception there is no need for a global trans-saccadic update, only the reference objects are used to assess stability. Indeed, it has been demonstrated that the saccade target region is more likely to be stored into trans-saccadic memory than other locations (Henderson & Hollingworth, 1999; Henderson & Hollingworth, 2003; Irwin, 1992; Irwin & Andrews, 1996; Irwin & Gordon, 1998) as also shown in a model simulation (Hamker, 2005b). Thus, the observed model RF dynamics which lead to an enhanced processing capacity at the saccade target region (for a detailed discussion regarding this topic please refer to Hamker et al., 2008), seem to support rather such a local conception of visual stability.

Recent psychophysical evidence for predictive remapping in humans seems to contradict this view. Melcher (2007) used the tilt aftereffect to assess predictive remapping. It was demonstrated that for an adaptor presented close to the fixation point just before a saccade, the tilt aftereffect is stronger at the future post-saccadic position of the adapted region than at the current adaptor position in visual space. This result was interpreted as evidence for remapping of receptive fields to their future position immediately before a saccade. It was further demonstrated that the tilt aftereffect is reduced for adaptors presented directly at the saccade target. However, evidence for predictive remapping in this case is rather limited. The RF shifts in our model are consistent with the transfer of the tilt aftereffect towards the future fixation position as tested experimentally and the reduced tilt aftereffect at the saccade target could be also explained by a processing of an increasing amount of unadapted cells whose RFs are shifted towards the saccade target prior to the eye movement.

To summarize, we provided evidence that most reported data of peri-saccadic RF shifts in extrastriate retinotcentric visual areas can be explained by a single mechanism, i.e. a preferred saccade target processing. However, it might be that a global remapping and a preferred saccade target processing operate in parallel in different brain areas. A global shift of RFs, as suggested by the theory of remapping, could be useful to stabilize a spatial percept of the scene, whereas the preferred processing of the saccade target area allows the brain to deal with the object of interest even before it is foveated. Thus, more detailed measurements of peri-saccadic RFs in both the ventral and dorsal pathway are needed in order to differentiate between the above mentioned possibilities and functional implications, and to improve our understanding of peri-saccadic perception and ultimately the subjective experience of visual stability.

Acknowledgments

F.H.H. was supported by the German Science Foundation DFG HA 2630/4-1, the German Federal Ministry of Education and Research project Visuo-spatial Cognition, and the EC Project FP7-ICT Eyeshots. M.L. was supported by the German Science Foundation DFG LA-952/3, the German Federal Ministry of Education and Research project Visuo-spatial Cognition, and the EC Projects Drivsco and Eyeshots.

References

Adams, D. L., & Horton, J. C. (2003). A precise retinotopic map of primate striate cortex generated from the representation of angioscotomas. *The Journal of Neuroscience, 23*, 3771–3789.

Armstrong, K. M., Fitzgerald, J. K., & Moore, T. (2006). Changes in visual receptive fields with microstimulation of frontal cortex. *Neuron, 50*, 791–798.

Armstrong, K. M., & Moore, T. (2007). Rapid enhancement of visual cortical response discriminability by microstimulation of the frontal eye field. *Proceedings of the National Academy of Sciences of the United States of America, 104*, 9499–9504.

Cavanaugh, J., & Wurtz, R. H. (2004). Subcortical modulation of attention counters change blindness. *The Journal of Neuroscience, 24*, 11236–11243.

Colby, C. L., & Goldberg, M. E. (1999). Space and attention in parietal cortex. *Annual Review of Neuroscience, 22*, 319–349.

Compte, A., & Wang, X. J. (2006). Tuning curve shift by attention modulation in cortical neurons: A computational study of its mechanisms. *Cerebral Cortex, 16*, 761–778.

Currie, C. B., McConkie, G. W., Carlson-Radvansky, L. A., & Irwin, D. E. (2000). The role of the saccade target object in the perception of a visually stable world. *Perception & Psychophysics, 62*, 673–683.

Deubel, H., Bridgeman, B., & Schneider, W. X. (1998). Immediate post-saccadic information mediates space constancy. *Vision Research, 38*, 3147–3159.

Deubel, H., & Schneider, W. X. (1996). Saccade target selection and object recognition: Evidence for a common attentional mechanism. *Vision Research, 36*, 1827–1837.

Deubel, H., Schneider, W. X., & Bridgeman, B. (1996). Postsaccadic target blanking prevents saccadic suppression of image displacement. *Vision Research, 36*, 985–996.

Duhamel, J. R., Colby, C. L., & Goldberg, M. E. (1992). The updating of the representation of visual space in parietal cortex by intended eye movements. *Science, 255*, 90–92.

Fischer, B., & Boch, R. (1981a). Selection of visual targets activates prelunate cortival cells in trained rhesus monkey. *Experimental Brain Research, 41*, 431–433.

Fischer, B., & Boch, R. (1981b). Enhanced activation of neurons in prelunate cortex before visually guided saccades of trained rhesus monkeys. *Experimental Brain Research, 44*, 129–137.

Godijn, R., & Pratt, J. (2002). Endogenous saccades are preceded by shifts of visual attention: Evidence from cross-saccadic priming effects. *Acta Psychologica, 110*, 83–102.

Hamker, F. H. (2003). The reentry hypothesis: Linking eye movements to visual perception. *Journal of Vision, 3*, 808–816.

Hamker, F. H. (2005a). The reentry hypothesis: The putative interaction of the frontal eye field, ventrolateral prefrontal cortex, and areas V4, IT for attention and eye movement. *Cerebral Cortex, 15*, 431–447.

Hamker, F. H. (2005b). A computational model of visual stability and change detection during eye movements in real world scenes. *Visual Cognition, 12*, 1161–1176.

Hamker, F. H., & Zirnsak, M. (2006). V4 receptive field dynamics as predicted by a systems-level model of visual attention using feedback from the frontal eye field. *Neural Networks, 19*, 1371–1382.

Hamker, F. H., Zirnsak, M., Calow, D., & Lappe, M. (2008). The peri-saccadic perception of objects and space. *PLoS Computational Biology, 4*(2), e31. doi:10.1371/journal.pcbi.0040031.

Henderson, J. M., & Hollingworth, A. (1999). The role of fixation position in detecting scene changes across saccades. *Psychological Science, 10*, 438–443.

Henderson, J. M., & Hollingworth, A. (2003). Eye movements and visual memory: Detecting changes to saccade targets in scenes. *Perception & Psychophysics, 65*, 58–71.

Hoffman, J. E., & Subramaniam, B. (1995). The role of visual attention in saccadic eye movements. *Perception & Psychophysics, 57*, 787–795.

Irwin, D. E. (1992). Memory for position and identity across eye movements. *Journal of Experimental Psychology. Learning, Memory, and Cognition, 18*, 307–317.

Irwin, D. E., & Andrews, R. (1996). Integration and accumulation of information across saccadic eye movements. In T. Inui & J. L. McClelland (Eds.), *Attention and performance XVI: Information integration in perception and communication* (pp. 125–155). Cambridge, MA: MIT Press.

Irwin, D. E., & Gordon, R. D. (1998). Eye movements, attention and trans-saccadic memory. *Visual Cognition, 5*, 127–155.

Irwin, D. E., McConkie, G. W., Carlson-Radvansky, L., & Currie, C. (1994). A localist evaluation solution for visual stability across saccades. *Behavioral and Brain Sciences, 17*, 265–266.

Kaiser, M., & Lappe, M. (2004). Perisaccadic mislocalization orthogonal to saccade direction. *Neuron, 41*, 293–300.

Kowler, E., Anderson, E., Dosher, B., & Blaser, E. (1995). role of attention in the programming of saccades. *Vision Research, 35*, 1897–1916.

Mazer, J. A., & Gallant, J. L. (2003). Goal-related activity in V4 during free viewing visual search: Evidence for a ventral stream visual salience map. *Neuron, 40*, 1241–1250.

McConkie, G. W., & Currie, C. B. (1996). Visual stability across saccades while viewing complex pictures. *Journal of Experimental Psychology. Human Perception and Performance, 22*, 563–581.

Melcher, D. (2007). Predictive remapping of visual features precedes saccadic eye movements. *Nature Neuroscience, 10*, 903–907.

Melcher, D., & Colby, C. L. (2008). Trans-saccadic perception. *Trends in Cognitive Sciences, 12*, 466–473.

Moore, T., & Armstrong, K. M. (2003). Selective gating of visual signals by microstimulation of frontal cortex. *Nature, 421*, 370–373.

Moore, T., Tolias, A. S., & Schiller, P. H. (1998). Visual representation during saccadic eye movements. *Proceedings of the National Academy of Sciences of the United States of America, 95*, 8981–8984.

Morrone, M. C., Ross, J., & Burr, D. C. (1997). Apparent position of visual targets during real and simulated saccadic eye movements. *The Journal of Neuroscience, 17*, 7941–7953.

Müller, J. R., Philiastides, M. G., & Newsome, W. T. (2005). Microstimulation of the superior colliculus focuses attention without moving the eyes. *Proceedings of the National Academy of Sciences of the United States of America, 102*, 524–529.

Mullette-Gillman, O. A., Cohen, Y. E., & Groh, J. M. (2005). Eye-centered, head-centered, and complex coding of visual and auditory targets in the intraparietal sulcus. *Journal of Neurophysiology, 94*, 2331–2352.

Nakamura, K., & Colby, C. L. (2002). Updating of the visual representation in monkey striate and extrastriate cortex during saccades. *Proceedings of the National Academy of Sciences of the United States of America, 99*, 4026–4031.

Peterson, M. S., Kramer, A. F., & Irwin, D. E. (2004). Covert shifts of attention precede involuntary eye movements. *Perception & Psychophysics, 66*, 398–405.

Pouget, P., Stepniewska, I., Crowder, E. A., Leslie, M. W., Emeric, E. E., Nelson, M. J., et al. (2009). Visual and motor connectivity and the distribution of calcium-binding proteins in macaque frontal eye field: Implications for saccade target selection. *Frontiers in Neuroanatomy, 3*, 2. doi:10.3389/neuro.05.002.2009.

Quaia, C., Optican, L. M., & Goldberg, M. E. (1998). The maintenance of spatial accuracy by the perisaccadic remapping of visual receptive fields. *Neural Networks, 11*, 1229–1240.

Ross, J., Morrone, M. C., & Burr, D. C. (1997). Compression of visual space before saccades. *Nature, 386*, 598–601.

Schall, J. D., Morel, A., King, D. J., & Bullier, J. (1995). Topography of visual cortex connections with frontal eye field in macaque: Convergence and segregation of processing streams. *The Journal of Neuroscience, 15*, 4464–4487.

Schira, M. M., Wade, A. R., & Tyler, C. W. (2007). Two-dimensional mapping of the central and parafoveal visual field to human visual cortex. *Journal of Neurophysiology, 97*, 4284–4295.

Shepherd, M., Findlay, J. M., & Hockey, R. J. (1986). The relationship between eye movements and spatial attention. *The Quarterly Journal of Experimental Psychology Section A, 38*(3), 475–491.

Sommer, M. A., & Wurtz, R. H. (2004). What the brain stem tells the frontal cortex. I. Oculomotor signals sent from superior colliculus to frontal eye field via mediodorsal thalamus. *Journal of Neurophysiology, 91*, 1381–1402.

Sommer, M. A., & Wurtz, R. H. (2006). Influence of the thalamus on spatial visual processing in frontal cortex. *Nature, 444*, 374–377.

Suzuki, S., & Cavanagh, P. (1997). Focussed attention distorts visual space: An attentional repulsion effect. *Journal of Experimental Psychology. Human Perception and Performance, 23*, 443–463.

Tolias, A. S., Moore, T., Smirnakis, S. M., Tehovnik, E. J., Siapas, A. G., & Schiller, P. H. (2001). Eye movements modulate visual receptive fields of V4 neurons. *Neuron, 29*, 757–767.

Umeno, M. M., & Goldberg, M. E. (1997). Spatial processing in the monkey frontal eye field. I. Predictive responses. *Journal of Neurophysiology, 78*, 1373–1383.

Ungerleider, L. G., Galkin, T. W., Desimone, R., & Gattass, R. (2008). Cortical connections of area V4 in the macaque. *Cerebral Cortex, 18*, 477–499.

Van Essen, D. C., Newsome, W. T., & Maunsell, J. H. (1984). The visual field representation in striate cortex of the macaque monkey: Asymmetries, anisotropies, and individual variability. *Vision Research, 24*, 429–448.

Walker, M. F., Fitzgibbon, E. J., & Goldberg, M. E. (1995). Neurons in the monkey superior colliculus predict the visual result of impending saccadic eye movements. *Journal of Neurophysiology, 73*, 1988–2003.

Womelsdorf, T., Anton-Erxleben, K., & Treue, S. (2008). Receptive field shift and shrinkage in macaque temporal area through attentional gain modulation. *The Journal of Neuroscience, 28*, 8934–8944.

Wurtz, R. H. (2008). Neuronal mechanism of visual stability. *Vision Research, 48*, 2070–2089.